

Oscillator Design and Fabrication using a Miniatured Hairpin Resonator

Jang-Gu Kim* · Sok-Kyun Han** · Hyung-Ha Choi***

*, ** Division of Marine Electronic & Comm. Eng., Mokpo National Maritime University, Mokpo 530-729, Korea

Abstract : In this papers, an S-band oscillator of the low phase noise property using a miniaturized micro-strip hairpin shaped ring resonator is presented. The substrate has a dielectric constant $\epsilon_r=3.5$, a thickness $h=0.508\text{ mm}$, and loss tangent $\tan\delta = 0.002$. A designed and fabricated oscillator shows low phase noise performance of 99.71 dBc/Hz at 100 KHz offset frequency and of output power 19.584 dBm at center frequency 2.450 GHz. This circuit was fabricated with hybrid technique, but can be fully compatible with the MMIC due to its entirely planar structure.

Key words : Oscillator, Phase noise, Hairpin shaped ring resonator, MMIC

1. Introduction

The fast growing commercial mobile radio communication markets of recent years has significantly increased the demand for low cost and low phase noise oscillator in the S band. A dielectric resonator of high Q is widely used for the low phase noise performance (Wilson P. G. and Carver R. D 1989; Hosoya K., Tanaka S., Amamiya Y., Niwa T., Shimawaki H., and Honjo K., 2000). However, the size of resonator is too large to design in the S band. And its three dimensional structure is not adequate for the monolithic microwave integrated circuits (MMIC). A planar type resonators have been developed to be applied in an MMIC and to improve the phase noise of an oscillator [2][3]. However, the total size of these circuits can be larger because the electrical lengths of resonator are nearly half wavelength, so this makes the cost of the MMIC higher.

Due to the advantages of higher yield properties size and easy fabrication, a planar micro-strip hairpin resonator has been drawing much attention. From the conventional half-wavelengths hairpin resonator to miniaturized hairpin resonator shown in Fig. 1, a size reduction of resonator has been dramatically achieved (Wilson P. G. and Carver R. D 1989; Ku J. T., Maa M. J., and Lu P. H.; Lee S. Y. and Tsai C. M., 2000). Fig. 1(c) shows a miniaturized hairpin shaped spilt ring resonator with open coupled line has an improved structure compared with lumped element capacitor in Fig. 1(b). This structure can also be applied to a much higher frequency range and is suitable for MIC's because of its photo etching manufacturing process. In this papers, an S-band oscillator of the low phase noise property using

miniaturized micro-strip hairpin shaped ring resonator is presented. This circuit was fabricated with hybrid technique, but can be fully compatible with the MMIC due to its entirely planar structure.

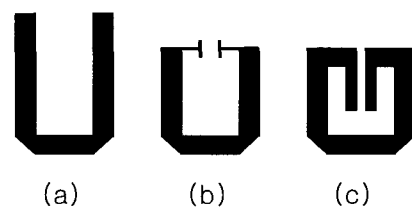


Fig. 1 Some structural variations of the hairpin resonator. (a) Conventional hairpin resonator. (b) Miniaturized hairpin resonator. (c) Miniaturized hairpin resonator having coupled lines.

2. Hairpin shaped spilt-ring resonator

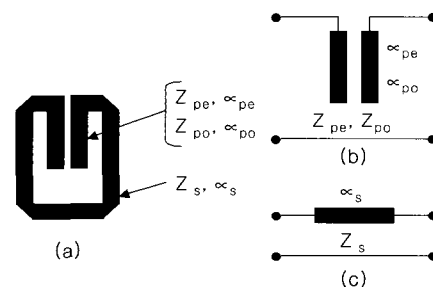


Fig. 2 Resonance conditions (a) Electrical parameters of the compact hairpin resonator. (b) Parallel coupled lines and their ABCD matrices. (c) Transmission line and their ABCD matrices.

* Corresponding Author : Jang-Gu Kim, jgkim9541@mmu.ac.kr 061)240-7121
 ** prohan@hanmail.net 061)240-7121
 *** antenna@mmu.ac.kr 061)240-7117

The resonance conditions of split ring resonator composed of a transmission line and a lumped element can be obtained using the $ABCD$ matrices, which express a transmission line and a capacitor, respectively. A miniaturized hairpin shaped split ring resonator with parallel coupled lines to replace the lumped element capacitor can be analyzed using following parameter as shown in Fig. 2(a)(Sagawa et al., 1989; Makimoto and Yamashita, 2000).

Z_s ; Characteristic impedance of the single line,

θ_s ; electrical length of the single line,

Z_{pe}, Z_{po} ; even and odd mode impedance of the parallel coupled lines,

θ_{pe}, θ_{po} ; even and odd mode electrical length of the parallel coupled lines.

Using these parameter, the $ABCD$ matrix for parallel coupled lines with an open end in Fig. 2(b) is given by

$$\begin{bmatrix} \frac{Z_{pe}\cot\theta_{pe} + Z_{po}\cot\theta_{po}}{Z_{pe}\cot\theta_{pe} - Z_{po}\cot\theta_{po}} & -j \frac{2Z_{pe}Z_{po}\cot\theta_{pe}\cot\theta_{po}}{Z_{pe}\cot\theta_{pe} - Z_{po}\cot\theta_{po}} \\ j \frac{2}{Z_{pe}\cot\theta_{pe} - Z_{po}\cot\theta_{po}} & \frac{Z_{pe}\cot\theta_{pe} + Z_{po}\cot\theta_{po}}{Z_{pe}\cot\theta_{pe} + Z_{po}\cot\theta_{po}} \end{bmatrix} \quad (1)$$

and the $ABCD$ matrix for single transmission in Fig. 2(c) is given by

$$\begin{bmatrix} \cos\theta_s & jZ_s\sin\theta_s \\ j\frac{\sin\theta_s}{Z_s} & \cos\theta_s \end{bmatrix} \quad (2)$$

The resonance condition can be calculated from the input admittance using the total $ABCD$ matrix. The results are as follows :

$$\begin{aligned} & (Z_{pe} - Z_{po}\cot\theta_{pe}\cot\theta_{po} - Z_s^2) \sin\theta_s \\ & + Z_s(Z_{pe}\cot\theta_{pe} + Z_{po}\cot\theta_{po}) \cos\theta_s \\ & - Z_s(Z_{pe}\cot\theta_{pe} - Z_{po}\cot\theta_{po}) = 0 \end{aligned} \quad (3)$$

when $\theta_{pe} = \theta_{po} = \theta_p$, Eg.(3) is simplified to

$$\begin{aligned} & (Z_{pe} - Z_{po}\cot\theta_p - Z_s^2\tan\theta_p) \sin\theta_s \\ & + Z_s(Z_{pe} + Z_{po}) \cos\theta_s \\ & - Z_s(Z_{pe} - Z_{po}) = 0 \end{aligned} \quad (4)$$

The resonance conditions expressed above are general descriptions derived from the input admittance of the resonator. However, as their relationship is too complicated

to allow an understanding of their physical meanings, the resonance conditions from viewpoint of equivalent circuits at resonance are needed in analyzing resonance characteristics. Parallel coupled lines with an open-circuited end are considered to have either an odd-mode or an even-mode electro-magnetic field distribution at resonance.

Therefore, two equivalent circuits must exist, as shown in Fig. 3. These resonators are found to be stepped impedance resonator (SIR'S)(Makimoto M. and Yamashita S., 1980), and their resonance conditions are as follows:

odd mode :

$$\tan(\theta_s/2) \cdot \tan\theta_p = K_o = Z_{po}/Z_s \quad (5)$$

even mode :

$$\tan(\theta_s/2) \cdot \tan\theta_p = K_e = Z_{pe}/Z_s \quad (6)$$

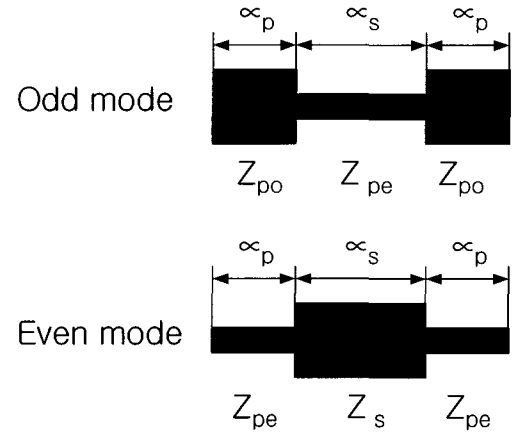


Fig. 3 Equivalent circuits at resonance points

The fundamental resonance frequency occurs in the odd mode, and the next higher resonance frequency (the lowest spurious frequency) in the even mode. In this way, higher mode resonance frequencies alternate odd and even. The equivalent circuits mentioned above are enough to facilitate analysis of the resonance frequencies of fundamental and the higher mode. The fundamental resonance frequency can be obtained by solving (eg.(5)), and its fine tuning can be easily achieved by adjusting the length of the parallel coupled line during manufacturing process.

3. Oscillator design theory

In the design of many oscillators, minimizing noise and maximizing output power are conflicting requirements. To achieve low noise, oscillators must operate well below the device's maximum output power capability. Fig. 4 shows

the schematic of a general three-terminal device oscillator. Γ_r is chosen such that the oscillation condition, Eq.(7) is satisfied, i.e.,

$$S'_{11} = 1/\Gamma_R \tag{7}$$

where,

$$S'_{11} = \frac{S_{11} + S_{12} S_{21} \Gamma_c}{1 - S_{22} \Gamma_c} \tag{8}$$

Oscillations will occur if s'_{11} is greater than unity: more energy is being reflected from the gate than is incident. The modified device resistance R_d will be negative over a range of frequencies dependent on the design of the feedback and resonator circuits.

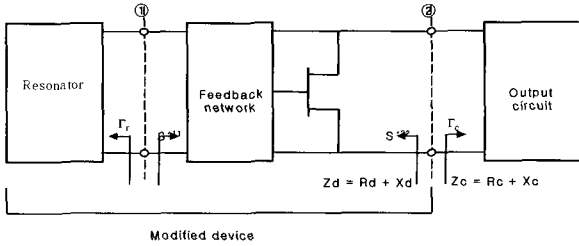


Fig. 4 MESFET Oscillator model

A small-signal design procedure for MESFET oscillators was introduced by Wilson and Carver [1], which will achieve steady-state oscillation at or near the start-up frequency based on the small-signal device model. and its linear design procedure is as follows :

- 1) Obtain a small-signal model of the device.
- 2) Design the feedback network to maximize S_{11} at the desired oscillation frequency.
- 3) Plot the input and output amplifier stability factors of the modified device on a smith chart.
- 4) Design a resonator circuit with Γ_r in the potentially unstable regions of the Smith chart at the desired frequency. For start-up, we require

$$|\Gamma_r| > 1/|S'_{11}| \tag{9}$$

$$\angle \Gamma_r = \angle \frac{1}{S'_{11}} \tag{10}$$

- 5) Design the output circuit so that any start-up:

$$X_c = -X_d, \tag{11}$$

$$R_c = -R_d/3 \tag{12}$$

at the design frequency[10]. After start up, R_d will decrease until $R_d = -R_c$. 6) Repeat steps 4) and 5) iteratively until conditions Eq.(11) and (12) are satisfied, and Γ_r and Γ_c are in the unstable regions of the smith chart.

The linear design approach cannot be used to maximize the output steady-state operation, an oscillating device exhibits large-signal behavior: its S-parameters vary with output power level. Because the linear model is independent of power level, we are unable to predict the steady-state output power level of the oscillator fundamental frequency or of any harmonics. Therefore, A harmonic balance for a nonlinear oscillator circuit is needed to predict a output power of fundamental frequency, harmonic frequencies, and phase noise.

4. Oscillator design and Measured results

Fig. 5 shows the layouts of a miniaturized hairpin shaped spilt ring resonator with parallel coupled line fabricated where the substrate has a dielectric constant $\epsilon_r = 3.5$, a thickness $h = 0.508 \text{ mm}$, and loss tangent $\tan \delta = 0.002$. The resonator design parameter are as follows($f = 2.450 \text{ GHz}$) : $Z_s = 50 \Omega$, $\theta_s = 135^\circ$, $Z_{pe} = 95 \Omega$, $Z_{po} = 69.6 \Omega$, $\theta_p = 24.6^\circ$. The lengths of the parallel coupled line (θ_p) were adjusted to keep the resonance frequency. Fig. 6 shows the measured result.

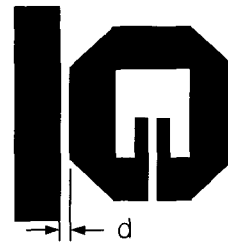


Fig. 5 Layout of the conventional miniaturized hairpin resonator

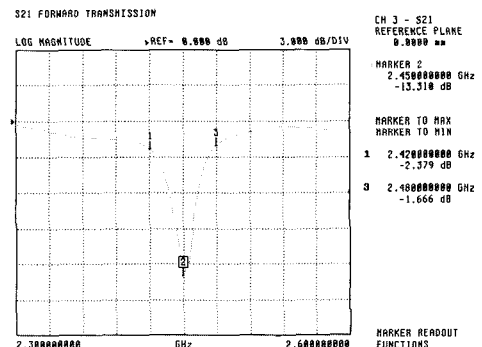


Fig. 6 Measured result of hairpin resonator

An oscillator incorporated with the miniaturized hairpin resonator was designed and fabricated using a AFT-54143 HEMT device with hybrid technique. This oscillator adopted series feedback topology and resonator was placed at the gate circuits with 50 ohm termination as shown in Fig. 7 and the spacing "d" is to couple the resonator to the micro-strip line, which effects output power and phase noise performance.

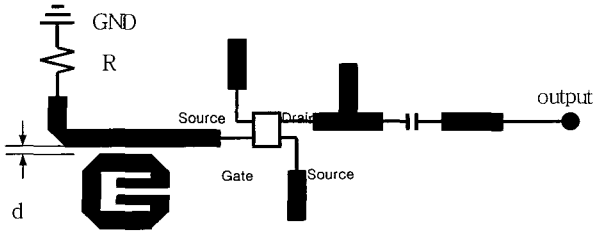


Fig. 7 Configuration of a miniaturized hairpin oscillator

The length of feedback stub line in the source port of the transistor were optimized in order to generate an enough negative resistance to compensate for the loss of the resonator. A linear small signal device model was used to ensure the start-up oscillation at the desirable frequency.

And Fig. 8 shows oscillation possibility in desirable frequency.

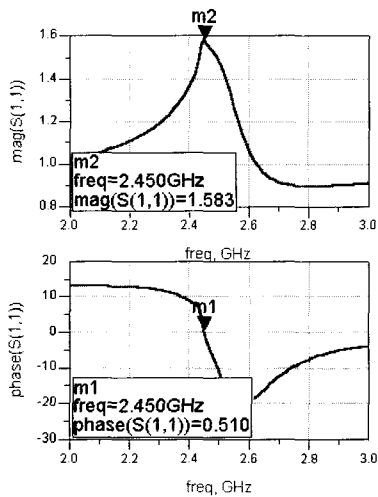


Fig. 8 Oscillation test

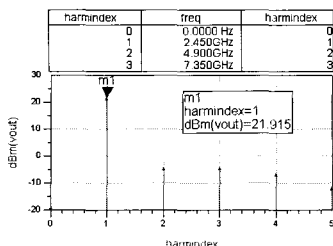


Fig. 9 Output characteristics

A curtice ADS model of transistor was used in harmonic balance simulation to more accurately predict output power and to optimize the phase noise. The output power of the oscillator signal and phase noise was also optimized by adjusting the resonator coupling to micro-strip line and matching circuitry while keeping harmonic components suppressed.

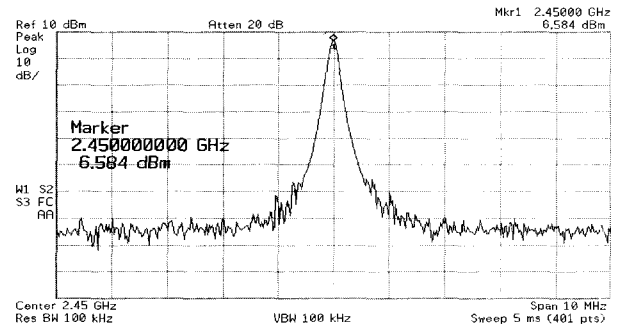


Fig. 10 Oscillator output power

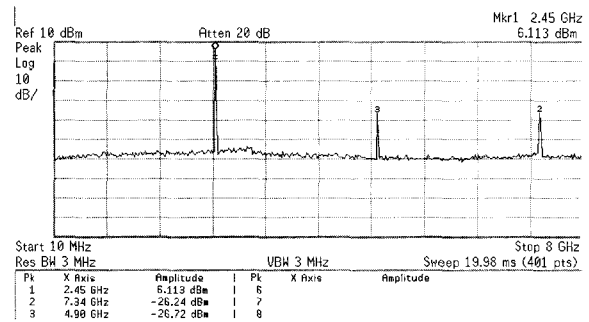


Fig. 11 Output power harmonics

The measured output spectrum for the fabricated oscillator is illustrated in Fig. 10. The oscillation frequency is 2.450 GHz, which is the resonant frequency and design frequency and it shows the output power of 19.584 dBm, considering 10 dB of attenuator and 3 dB of cable loss. The harmonic suppression exhibits 32.353 dB, as shown in Fig. 11. Also, the phase noise performance is 99.71 dBc/Hz at 100KHz offset, as shown in Fig. 12.

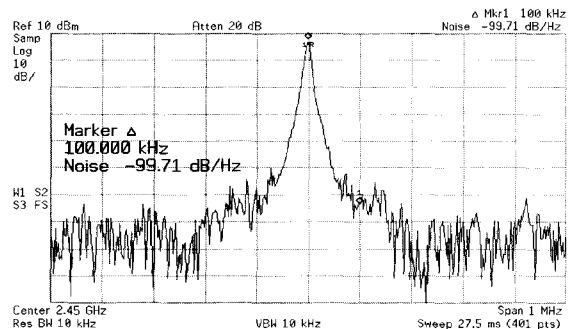


Fig. 12 Measured phase noise

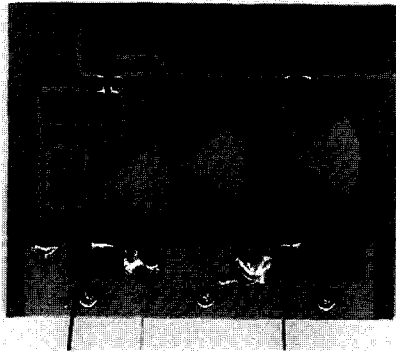


Fig. 13 Fabricated picture oscillator

5. Conclusion

A low phase noise and high power oscillator using a miniaturized hairpin shaped split ring resonator has been designed and fabricated. This approach can be fully integrated in an MMIC due to its planar structure. The designed and fabricated 2.450 GHz oscillator shows low phase performance of -99.71 dBc/Hz a 100KHz offset and of output power 19.584 dBm at center frequency 2.450 GHz. Due to its simple planar structure, it is expected that this technique can be effectively used for low cost, low phase noise MMIC oscillators.

References

[1] Gonzalez, G.(1984), *Microwave transistor Amplifiers Analysis and Design*, PrenticeHall.
 [2] Hyun, A. S., Kim, H. S., Park, J. Y., Kim, J. H., Lee, J. C., Kim, N. Y., Kim, B. K., and Hong, U. S.(1999), "K-band hair-Pin resonator oscillators," *IEEE MTT-S Dig.*, pp. 725-728.

[3] Hosoya, K., Tanaka, S., Amamiya, Y., Niwa, T., Shimawaki, H., and Honjo, K.(2000), "A low phase-noise 38-GHz HBT MMIC oscillator utilizing a novel transmission line resonator," *IEEE MTT-S Dig.*, pp. 47-50.
 [4] Ku, J. T., Maa, M. J., and Lu, P. H.(2000), "A microstrip elliptic function filter with compact miniaturized hairpin resonator," *IEEE Microwave Guided Wave Lett.*, vol. 10, pp. 94-95.
 [5] Lee, Y. T., Lim, J. S., Kim, C. S.(2002), "A Compact-Size Microstrip Spiral Resonator and Its Application to Microwave Oscillator," *IEEE Microwave and wireless Components Letters*, Vol. 12, No. 10. October pp. 375-377.
 [6] Lee, S. Y. and Tsai, C. M.(2000), "New cross-coupled filter design using improved hairpin resonators," *IEEE trans. MTT*, Vol. 44, pp. 2482-2490.
 [7] Makimoto, M. and Yamashita, S.(2000), *Microwave Resonator and Filters for Wireless communication*, Springer.
 [8] Makimoto, M. and Yamashita, S.(1980), "Bandpass filters using parallel coupled stripline stepped impedance resonators", *IEEE trans. MTT*, vol 28, pp. 1413+-1417.
 [9] Sagawa, M., Takahashi, K., and Makimot, M.(1989), "Miniaturized hairpin resonator filters and their application to receiver front-end MIC's," *IEEE trans. MTT*, vol. 37, pp. 1991-1997.
 [10] Wilson, P. G. and Carver, R. D.(1989), "An easy-to-use FET DRO design procedure suited to most CAD programs," in *1989 IEEE MTT-S Dig.*, pp. 1033-1036.

Received 30 April 2004

Accepted 7 June 2004